

**NOTE: This is the peer reviewed version of the following article:**

*„Programming photo-response in liquid crystal polymer actuators with laser projector“,*

**which has been published in final form at**  
**[\[http://doi.org/10.1002/adom.201700949\]](http://doi.org/10.1002/adom.201700949).**

**This article may be used for non-commercial purposes in accordance with Wiley Terms and Conditions for Use of Self-Archived Versions.**

DOI: 10.1002/ ((please add manuscript number))

Article type: Full Paper

## Programming photo-response in liquid crystal polymer actuators with laser projector

*Owies M. Wani,<sup>a</sup> Hao Zeng,<sup>\*a</sup> Piotr Wasylczyk<sup>b</sup> and Arri Priimagi<sup>\*a</sup>*

O. M. Wani, Dr. H. Zeng and Prof. A. Priimägi  
Laboratory of Chemistry and Bioengineering, Tampere University of Technology, P.O. Box  
541, FI 33101 Tampere, Finland

Dr. P. Wasylczyk

Photonic Nanostructure Facility, Institute of Experimental Physics, Faculty of Physics,  
University of Warsaw, ul. Pasteura 5, 02-093 Warsaw, Poland.

**Keywords:** photoalignment, photoactuation, liquid crystal, azobenzene, laser projector, patterning

**Abstract.** We demonstrate a versatile, laser-projector-based method for programming alignment patterns into monolithic films of liquid crystal polymer networks. Complex images can be photopatterned into the polymer films with sub-100- $\mu\text{m}$  resolution, using relatively short exposure times. The method is further used to devise both photochemically and photothermally driven actuators that can undergo distinct light-induced shape changes, dictated by the programmed alignment patterns. Deformation modes such as buckling and coiling, as well as miniature robotic devices such as a gripper and a light-responsive octopod, are demonstrated. The reported technique enables easy and cost-effective programmable actuation with relatively high throughput, thus significantly facilitating the design and realization of functional soft robotic actuators.

## 1. Introduction

Smart materials that can change their properties in response to external conditions are at the forefront of contemporary materials research.<sup>[1–3]</sup> Stimuli-responsive soft actuators represent an important sub-class among such materials.<sup>[4–6]</sup> Potential applications of the soft actuators include artificial muscles,<sup>[7]</sup> tissue engineering,<sup>[8]</sup> biotechnologies,<sup>[9]</sup> microrobotics,<sup>[10]</sup> micro-optics,<sup>[11]</sup> etc. The key to building up a functional micro-system based on soft actuators is to program the material to achieve multiple desired deformations. Programming soft actuators, however, is challenging as they lack individual control circuitry (often adopted in conventional electronic actuators), restricted by their miniature sizes. Hence, programmable soft materials that can exhibit multiple deformations and thus perform a variety of tasks, are in great demand.

Liquid crystal polymer networks (LCNs; note that we use this term to describe both elastomeric and glassy polymer networks) have emerged as promising materials for fabricating soft actuators.<sup>[12–14]</sup> LCNs combine the anisotropy of the constituent liquid-crystal (LC) molecules and the elasticity of polymer networks, and are capable of stimuli-responsive shape-change at the macroscopic scale. LCNs can be actuated by various stimuli such as light,<sup>[15]</sup> heat,<sup>[16]</sup> solvent,<sup>[17]</sup> and humidity.<sup>[18]</sup> Being a clean, remote and precisely controllable stimulus, light is a particularly attractive energy source.<sup>[19]</sup> The light-triggered deformation of an LCN actuator is governed by the alignment distribution of the constituent liquid-crystal molecules within the polymer network, and developing methods for precise control over the director distribution in order to obtain desired photoactuation mode is an important topic of research.<sup>[14,20–22]</sup>

Photoalignment has proven to be a successful technique in patterning complex alignments into liquid-crystalline materials<sup>[23–25]</sup> and in devising on-demand actuations into LCNs.<sup>[21]</sup> The technique is based on illuminating a thin photoresponsive layer, a

“command surface”,<sup>[26]</sup> with linearly polarized light. Upon illumination, the photoalignment layer becomes anisotropic, thereby changing the boundary conditions experienced by the liquid-crystal molecules in the vicinity, and forcing them to align either perpendicular<sup>[27]</sup> or parallel<sup>[28]</sup> to the light polarization. Photopatterning of director orientation can be achieved by spatially modulating the light polarization,<sup>[27]</sup> or exposure through mask(s).<sup>[28,29]</sup> White and colleagues have used a laser setup to raster scan a focussed laser beam with controlled polarization across the sample, and thus achieved local control in the director distribution.<sup>[30–32]</sup> Also spatial light modulators and digital micromirror devices have been used for high-throughput patterning.<sup>[17,33–35]</sup> These demonstrations require either pre-patterned masks or relatively complex optical set-ups for programming the desired director distribution.

Herein, we use a laser projector with a microelectromechanical system (MEMS) - based scanning mirror assembly (PICO®, Sony) to program the liquid-crystal alignment within a monolithic LCN film. Photopatterning is achieved by projecting an arbitrary computer-generated image onto the photoalignment layer, using pre-defined light polarization. The projector is capable of addressing a minimum feature size of 50  $\mu\text{m}$  over an area of  $25 \times 14 \text{ mm}^2$ . A series of complex photoactuators, such as defect buckling, coiling strip with gradient in pitch, four-arm gripper, and bi-directional bending in an octopod, are demonstrated by engineering different director orientations via photopatterning. The photoactuators are fabricated by polymerizing LC monomer mixtures inside LC cells that have been fabricated using the photoalignment-patterned glass substrates, opening the LC cells, and finally peeling off the polymerized films to yield free-standing actuators.

## 2. Results and Discussion

The working principle of the laser projector is schematically illustrated in **Figure 1a**. The device contains three time-modulated laser diodes (red 650 nm, green 550 nm and

blue 445 nm) scanned with the MEMS single micro-mirror. By repetitive horizontal and vertical scanning, the device is able to project images with  $1799 \times 799$  pixel resolution at 60 Hz.<sup>[36]</sup> To match the absorption band of the photoalignment material (Brilliant Yellow, **8** in **Figure 3**),<sup>[37]</sup> we only used the blue laser diode for photopatterning. Before illuminating the alignment layer, a rotating linear polarizer was used to control the light polarization direction (and thus the molecular alignment direction, which is in the plane of the sample and perpendicular to the light polarization), and a lens ( $f=30$  mm) projected the image onto the sample plane. The image shown in **Figure 1b** (from a Finnish video game franchise the Angry Birds, by Rovio Entertainment Ltd.) was projected on a glass slide coated with the alignment layer (details in Materials and Methods Section), followed by projection of its inverted (negative) image with  $45^\circ$  difference in the polarization direction. After photopatterning, a thin layer of LC monomer mixture, consisting of 99 wt% LC diacrylate **3**, and 1 wt % of photoinitiator **7**, was spin-coated and polymerized on the slide for the alignment visualization (see Figure 3 for chemical structures). **Figure 1c** and **1d** show the cross-polarized images, where the sample is placed at  $0$  and  $45^\circ$  angle with respect to the polarizers, respectively, illustrating that the image can be successfully patterned onto the LCN film.

**Figure 2a** shows the minimum line widths of patterned structures, which are  $\approx 50$   $\mu\text{m}$  in the horizontal and  $\approx 75$   $\mu\text{m}$  in the vertical direction. The difference is due to the lateral scanning direction of the micro-mirror. To determine the minimum pixel size of two-dimensional patterning, we projected checkerboard patterns of different size onto the sample and obtained a minimum period of  $100 \times 100$   $\mu\text{m}^2$  (**Figure 2b**). To assess the time needed for efficient photoalignment, we measured the evolution of the dichroic ratio of molecule **6**, doped in the visualization layer (see previous paragraph), as a function of time (**Figure S1**). As can be seen in **Figure 2d**, the dichroic ratio saturates after 5-minute exposure, indicating that 5 min suffices

to inscribe one image. The light intensity on the sample plane being  $3.0 \text{ mW}\cdot\text{cm}^{-2}$ , this corresponds to the absorbed energy below  $1 \text{ J}/\text{cm}^{-2}$ .

To demonstrate the utility of the photoalignment patterns in devising macroscopic LCN photoactuators, we used two polymerizable mixtures (**A** and **B**; see Figure 3 for the chemical structures). Mixture **A** contained 53 mol % of monomer **1**, 18 mol % of monomer **2**, 21 mol % of crosslinker **4**, 7 mol % of azobenzene crosslinker **5**, and 1 mol % of photoinitiator **7**. Mixture **B** consisted of 77 mol % of monomer **1**, 20 mol % of crosslinker **3**, 2 mol % of azobenzene dopant **6**, and 1 mol % of photoinitiator **7**. UV-Vis absorption spectra of the azobenzene molecules **5** and **6** are given in Figure S2. Mixture **A** undergoes photoactuation via photochemical, *trans-cis* isomerization-driven, mechanism,<sup>[38]</sup> while in mixture **B** the actuation is driven by photothermal effects.<sup>[27]</sup> The difference in the actuation mechanisms results from (i) the fact that mixture **A** contains azobenzene crosslinks while the azobenzenes are simply doped into mixture **B**, and (ii) the different lifetimes of the *cis*-isomers of **5** and **6**, which are in the order of hours and seconds, respectively. The long *cis*-lifetime of **5** preserves the deformed structure even after turning off the light, while it can return to the original shape by absorbing another wavelength or via thermal relaxation in relatively long time.<sup>[39]</sup> In **6**, short *cis*-lifetime/fast thermal relaxation enable continuous *trans-cis-trans* cycling upon illumination, thus efficiently transferring the photon energy into heat.<sup>[40]</sup> In azobenzene-based actuators, these two mechanisms cannot be completely de-coupled, yet dominance of one mechanism over the other can lead to very distinct actuation behaviour. For example, shape-persistent actuators based on *trans-cis* isomerization of fluorinated azobenzene crosslinkers yield bi-stable actuators,<sup>[41]</sup> while photothermal actuators are the preferred approach when developing high-frequency, light-driven photomechanical oscillators<sup>[42]</sup> and miniature robots.<sup>[15,40]</sup>

Both mixtures **A** and **B** are adaptable to photoalignment with the laser projector, and we applied four kinds of alignment patterns to demonstrate different actuation possibilities. All the actuators are of 50  $\mu\text{m}$  thickness, unless otherwise stated. Mixture **A** was used to fabricate films with alignment patterns shown in **Figure 4a** and **4e**. The pattern in Figure 4a corresponds to a +1 topological defect in the LC orientation,<sup>[43]</sup> where molecules in the bulk of the film are aligned in the planar square geometry. Such alignment results in cone/anti-cone buckling deformation upon illumination with UV light (385 nm, 130  $\text{mW cm}^{-2}$ , exposure time 1.5 min), while the initial shape is recovered upon exposure to visible light (460 nm, 150  $\text{mW cm}^{-2}$ , 1 min), as illustrated in **Figure 4b**, **4c**, and **4d** (see also **video S1**). The conical initial shape of the film, seen in Figure 4b, can be explained by residual stress generated in the LCN film during photopolymerization.<sup>[44–46]</sup> Figure 4e represents an LCN strip with end-to-end gradient in director orientation on one side of the film, *i.e.*, the director angle gradually varies from  $45^\circ$  on one end to  $15^\circ$  on the other end, with respect to the stripe direction. On the other side of the film, the molecules are aligned homeotropically. Upon actuation with UV light (385 nm, 130  $\text{mW cm}^{-2}$ , 1 min), the strip deforms into a coil with the pitch tapered along the body length: large pitch on the  $45^\circ$ -orientated end and small one at the  $15^\circ$  end, thus showing the possibility of programming a pitch gradient into a monolithic coiling strip.<sup>[38,46]</sup> The strip uncoils upon visible-light irradiation (460 nm, 150  $\text{mW cm}^{-2}$ , 1 min). The coiling/uncoiling is illustrated in **Figure 4f**, **4g**, and **4h**, and **video S2**.

Mixture **B** was used to fabricate films with alignment patterns shown in **Figure 4i** and **4m**. The pattern in Figure 4i defines a splay-aligned gripper structure, where one surface has planar boundary conditions directed along each arm, and the other surface has homeotropic anchoring. **Figure 4j**, **4k**, and **4l** show the photothermal actuation of thus patterned actuator upon 460 nm illumination (150  $\text{mW cm}^{-2}$ , 1.5 s), where the four arms bend towards the centre of the structure, performing a closing/gripping actuation. As

soon as the light is turned off, the arms return to their initial shape (**Video S3**). The final structure to demonstrate is an 8-legged octopod, schematically shown in Figure 4m. Each leg has a 90° twisted nematic alignment across the sample thickness, while adjacent legs have alternated director alignment orientations. Molecular orientation on the other surface is perpendicular to the one shown in Figure 4m. Upon illumination with 460 nm light (150 mW cm<sup>-2</sup>, 4 s), the adjacent legs bend into opposite directions, dictated by the alternating director alignment (**Figure 4n, 4o, 4p, video S4**). Such structure acts as a starting point for the fabrication of monolithic LCN octopods, and ultimately lead to light-controlled robots capable of walking locomotion.

### 3. Conclusions

We have demonstrated a facile method based on a portable laser projector to program alignment patterns into monolithic films of liquid crystal polymer networks using photoalignment layers. Single mirror MEMS laser projector is capable of patterning molecular orientation into the polymer networks with the minimum feature size of 50 μm over an area of 25 x 14 mm<sup>2</sup>. Four types of alignment patterns were inscribed to yield polymeric actuators with versatile light-driven deformations using both photochemical and photothermal mechanisms. We believe this work to widen the scope of shape-programmable liquid crystal polymer actuators, in particular enabling efficient and easy fabrication of smart microdevices and microrobots.

### 4. Experimental Section

**Preparation of the Angry Birds pattern.** A pre-cleaned glass slide (sonication in acetone and isopropyl alcohol for 20 minutes each, UV ozone treatment for 20 minutes) was spin coated with 0.5 wt % solution of Brilliant yellow (Sigma) in DMF (1500 rpm, 1 min), followed by baking at 90 °C on a hot plate for 15-20 min. After that, the sample was fixed in a holder placed in front of projector (Sony MP-CL1A mobile projector) and exposed to the projected Angry



Birds images (original and inverted) one after the other, 5 min each. Polarization difference of 45° was imparted between the original and inverted images. The photoalignment-patterned surface was then spin coated (2000 rpm; 500 rpm s<sup>-1</sup>; 1 min) with a LC mixture consisting of 99 wt% LC diacrylate monomer 1,4-Bis-[4-(3-acryloyloxypropyloxy)benzoyloxy]-2-methylbenzene 3 (Synthon chemicals) and 1 wt % photoinitiator Bis(2,4,6-trimethylbenzoyl)-phenylphosphineoxide (Sigma Aldrich) dissolved in chloroform (4 wt % solids). The spin coated layer was liquid crystalline at room temperature and was immediately polymerized under N<sub>2</sub> atmosphere using UV 375 nm LED (Thorlabs, 40 mW cm<sup>-2</sup>). Finally, the sample was analyzed between two polarizers and optical images were recorded.

**Resolution and time required for patterning.** For resolution studies, lines and checkerboards were projected onto a sample prepared in the same way as described above. For exposure time studies, substrates coated with the alignment layer were subjected to linearly polarized light from the projector for irradiation times of 0, 1, 2, 5, 10, 15 and 20 min. After photopatterning, the substrates were spin coated with a monomer mixture solution containing 97 wt % of the LC diacrylate 3, 2 wt % of Disperse red 1 (Sigma Aldrich), and 1 wt % of the UV photoinitiator, dissolved in chloroform (4 wt % solids). The spin-coated layer was polymerized under N<sub>2</sub> atmosphere using 375 nm LED (40 mW cm<sup>-2</sup>). Finally, polarized UV-vis absorption spectra were measured and are shown in Figure S1. Dichroic ratio of Disperse Red 1 molecule is calculated by using formula:

$$D = \frac{A_{\parallel}}{A_{\perp}},$$

where  $A_{\parallel}$  is the absorbance in the direction parallel to director axis, and  $A_{\perp}$  is the absorbance perpendicular to the director axis.

**Pre-programming actuation.** The photoalignment layers were prepared in the way described above, after which two photoalignment-coated substrates were made into an LC cell for photopatterning planar LCN films using 50 μm micro-spheres as spacers. In case of splay-

aligned films one of the glasses forming the LC cell was coated with homeotropic-aligning polyimide layer (JSR OPTMER, 3000 RPM, 1 min). The cell was then fixed on a holder placed in front of the projector, and patterning was carried out over an area of  $25 \times 14 \text{ mm}^2$ . Computer-controlled images with different brightness distribution were projected on the sample area, while the polarization was controlled by manually rotating the linear polarizer placed in between sample and projector. A 30-mm lens (Plano-Convex) was attached to polarizer to enhance the image sharpness at the sample plane. In case of twisted alignment, two glasses were patterned separately and covered (spin-coated) with liquid crystal monomer layer (polymerized immediately after spin-coating). The glasses were then glued to form an LC cell matching those patterns on two sides. In all LC cells,  $50 \text{ }\mu\text{m}$  spacers were used, except the one with modified director angle (Figure 4e-h), where  $10 \text{ }\mu\text{m}$  spacers were used. Polymerization of both mixtures was done by first heating the mixtures above the clearing point ( $80 \text{ }^\circ\text{C}$ ) and then subsequently, infiltrating them into LC cells on a hot plate, via capillary force. The cells were then brought to LC phase by cooling them to  $55 \text{ }^\circ\text{C}$  ( $5 \text{ }^\circ\text{C min}^{-1}$ ), using Linkam temperature-controlled stage. After that, mixture **A** was polymerized using  $420 \text{ nm}$  LED ( $70 \text{ mW cm}^{-2}$ ) and mixture **B** with  $375 \text{ nm}$  LED ( $40 \text{ mW cm}^{-2}$ ) for about 15 minutes each. Finally, cells were opened using a razor blade and the LCN films were cut into desired shapes. Normalized UV-vis spectra of the photoresponsive molecules present in mixtures **A** and **B** are given in Figure S2. Actuation of the films was performed using unpolarized UV  $385 \text{ nm}$  ( $130 \text{ mW cm}^{-2}$ ) and/or Visible  $460 \text{ nm}$  ( $150 \text{ mW cm}^{-2}$ ) light from a multichannel LED (Prior Scientific).

### Supporting Information

Supporting Information is available from the Wiley Online Library or from the author.

### Acknowledgements

A.P. gratefully acknowledges the financial support of the European Research Council (Starting Grant project PHOTOTUNE; Agreement No. 679646). O.M.W. is thankful to the graduate

school of Tampere University of Technology (TUT), and H.Z. to the TUT postdoctoral fellowship program, for supporting this work.

### Conflict of Interest

The authors declare no conflict of interest.

Received: ((will be filled in by the editorial staff))  
Revised: ((will be filled in by the editorial staff))  
Published online: ((will be filled in by the editorial staff))

### References

- [1] M. A. C. Stuart, W. T. S. Huck, J. Genzer, M. Müller, C. Ober, M. Stamm, G. B. Sukhorukov, I. Szleifer, V. V. Tsukruk, M. Urban, F. Winnik, S. Zauscher, I. Luzinov, S. Minko, *Nat. Mater.* **2010**, *9*, 101.
- [2] D. Roy, J. N. Cambre, B. S. Sumerlin, *Prog. Polym. Sci.* **2010**, *35*, 278.
- [3] P. M. Mendes, A. J. Downard, A. Muscroft-Taylor, A. D. Abell, T. Takagi, M. Kameda, T. Shinbo, T. Kanamori, Y. Yoshimi, J. F. Stoddart, *Chem. Soc. Rev.* **2008**, *37*, 2512.
- [4] L. Hines, K. Petersen, G. Z. Lum, M. Sitti, *Adv. Mater.* **2017**, *29*, 1603483.
- [5] F. Ilievski, A. D. Mazzeo, R. F. Shepherd, X. Chen, G. M. Whitesides, *Angew. Chemie Int. Ed.* **2011**, *50*, 1890.
- [6] O. M. Wani, H. Zeng, A. Priimagi, *Nat. Commun.* **2017**, *8*, 15546.
- [7] T. Mirfakhrai, J. D. W. Madden, R. H. Baughman, *Mater. Today* **2007**, *10*, 30.
- [8] F. Rosso, G. Marino, A. Giordano, M. Barbarisi, D. Parmeggiani, A. Barbarisi, *J. Cell. Physiol.* **2005**, *203*, 465.
- [9] M. Sitti, H. Ceylan, W. Hu, J. Giltinan, M. Turan, S. Yim, E. Diller, *Proc. IEEE* **2015**, *103*, 205.
- [10] M. Sitti, *Nature* **2009**, *458*, 1121.

- [11] T. Hirai, T. Ogiwara, K. Fujii, T. Ueki, K. Kinoshita, M. Takasaki, *Adv. Mater.* **2009**, *21*, 2886.
- [12] C. Ohm, M. Brehmer, R. Zentel, *Adv. Mater.* **2010**, *22*, 3366.
- [13] G. Fernández, *Nat. Mater.* **2012**, *12*, 12.
- [14] a) T. J. White, D. J. Broer, *Nat. Mater.* **2015**, *14*, 1087.  
b) Q. Li, *Intelligent Stimuli-Responsive Materials : From Well-Defined Nanostructures to Applications*, John Wiley & Sons, Hoboken, NJ, **2013**.  
c) H. K. Bisoyi, Q. Li, *Chem. Rev.* **2016**, *116*, 15089.
- [15] H. Zeng, O. M. Wani, P. Wasylczyk, A. Priimagi, *Macromol. Rapid Commun.* **2017**, DOI 10.1002/marc.201700224.
- [16] G. N. Mol, K. D. Harris, C. W. M. Bastiaansen, D. J. Broer, *Adv. Funct. Mater.* **2005**, *15*, 1155.
- [17] J. M. Boothby, T. H. Ware, *Soft Matter* **2017**, *13*, 4349.
- [18] M. Dai, O. T. Picot, J. M. N. Verjans, L. T. de Haan, A. P. H. J. Schenning, T. Peijs, C. W. M. Bastiaansen, *ACS Appl. Mater. Interfaces* **2013**, *5*, 4945.
- [19] T. J. White, *Photomechanical Materials, Composites, and Systems : Wireless Transduction of Light into Work*, John Wiley & Sons, Ltd, **2017**.
- [20] L. T. De Haan, A. P. H. J. Schenning, D. J. Broer, *Polym. (United Kingdom)* **2014**, *55*, 5885.
- [21] B. A. Kowalski, T. C. Guin, A. D. Auguste, N. P. Godman, T. J. White, *ACS Macro Lett.* **2017**, *6*, 436.
- [22] H. Zeng, P. Wasylczyk, G. Cerretti, D. Martella, C. Parmeggiani, D. S. Wiersma, *Appl. Phys. Lett.* **2015**, *106*, 1.
- [23] a) T. Seki, *Polym. J.* **2014**, *46*, 751.  
b) A. Martinez, H. C. Mireles, I. I. Smalyukh, *Proc. Natl. Acad. Sci. U. S. A.* **2011**, *108*, 20891.

- [24] O. Yaroshchuk, Y. Reznikov, T. Galstian, O. Yaroshchuk, A. Checco, V. Lazarev, S. Palto, S. Lee, K.-J. Han, S.-H. Jang, *J. Mater. Chem.* **2012**, *22*, 286.
- [25] B. Wei, W. Hu, Y. Ming, F. Xu, S. Rubin, J. Wang, V. Chigrinov, Y. Lu, *Adv. Mater.* **2014**, *26*, 1590.
- [26] K. Ichimura, *Chem. Rev.* **2000**, *100*, 1847.
- [27] H. Zeng, O. M. Wani, P. Wasylczyk, R. Kaczmarek, A. Priimagi, *Adv. Mater.* **2017**, DOI 10.1002/adma.201701814.
- [28] L. T. De Haan, C. Sánchez-Somolinos, C. M. W. Bastiaansen, A. P. H. J. Schenning, D. J. Broer, *Angew. Chemie - Int. Ed.* **2012**, *51*, 12469.
- [29] L. T. De Haan, V. Gimenez-Pinto, A. Konya, T. S. Nguyen, J. M. N. Verjans, C. Sánchez-Somolinos, J. V. Selinger, R. L. B. Selinger, D. J. Broer, A. P. H. J. Schenning, *Adv. Funct. Mater.* **2014**, *24*, 1251.
- [30] T. H. Ware, M. E. McConney, J. J. Wie, V. P. Tondiglia, T. J. White, *Science (80- )*. **2015**, *347*, 982.
- [31] M. E. McConney, A. Martinez, V. P. Tondiglia, K. M. Lee, D. Langley, I. I. Smalyukh, T. J. White, *Adv. Mater.* **2013**, *25*, 5880.
- [32] S. K. Ahn, T. H. Ware, K. M. Lee, V. P. Tondiglia, T. J. White, *Adv. Funct. Mater.* **2016**, *26*, 5819.
- [33] C. Culbreath, N. Glazar, H. Yokoyama, *Rev. Sci. Instrum.* **2011**, *82*, 2011.
- [34] H. Wu, W. Hu, H. Hu, X. Lin, G. Zhu, J.-W. Choi, V. Chigrinov, Y. Lu, *Opt. Express* **2012**, *20*, 16684.
- [35] B. A. Kowalski, V. P. Tondiglia, T. Guin, T. J. White, *Soft Matter* **2017**, *13*, 4335.
- [36] M. Freeman, M. Champion, S. Madhavan, *Opt. Photonics News* **2009**, *20*, 28.
- [37] O. Yaroshchuk, H. Gurumurthy, V. G. Chigrinov, H. S. Kwok, H. Hasebe, H. Takatsu, *Proc. IDW* **2007**, *7*, 1665.

- [38] S. Iamsaard, S. J. Aßhoff, B. Matt, T. Kudernac, J. J. L. M. Cornelissen, S. P. Fletcher, N. Katsonis, *Nat. Chem.* **2014**, *6*, 229.
- [39] M. Yamada, M. Kondo, J. Mamiya, Y. Yu, M. Kinoshita, C. Barrett, T. Ikeda, *Angew. Chemie Int. Ed.* **2008**, *47*, 4986.
- [40] A. H. Gelebart, D. J. Mulder, M. Varga, A. Konya, G. Vantomme, E. W. Meijer, R. L. B. Selinger, D. J. Broer, **2017**, DOI 10.1038/nature22987.
- [41] S. Iamsaard, E. Anger, S. J. ABhoff, A. Depauw, S. P. Fletcher, N. Katsonis, *Angew. Chemie - Int. Ed.* **2016**, *55*, 9908.
- [42] T. J. White, N. V. Tabiryan, S. V. Serak, U. A. Hrozhyk, V. P. Tondiglia, H. Koerner, R. A. Vaia, T. J. Bunning, *Soft Matter* **2008**, *4*, 1796.
- [43] C. D. Modes, M. Warner, *Phys. Rev. E - Stat. Nonlinear, Soft Matter Phys.* **2011**, *84*, 1.
- [44] C. L. Van Oosten, D. Corbett, D. Davies, M. Warner, C. W. M. Bastiaansen, D. J. Broer, *Macromolecules* **2008**, *41*, 8592.
- [45] K. Kumar, C. Knie, D. Bléger, M. A. Peletier, H. Friedrich, S. Hecht, D. J. Broer, M. G. Debije, A. P. H. J. Schenning, *Nat. Commun.* **2016**, *7*, 11975.
- [46] Y. Sawa, F. Ye, K. Urayama, T. Takigawa, V. Gimenez-Pinto, R. L. B. Selinger, J. V. Selinger, *Proc. Natl. Acad. Sci. U. S. A.* **2011**, *108*, 6364.

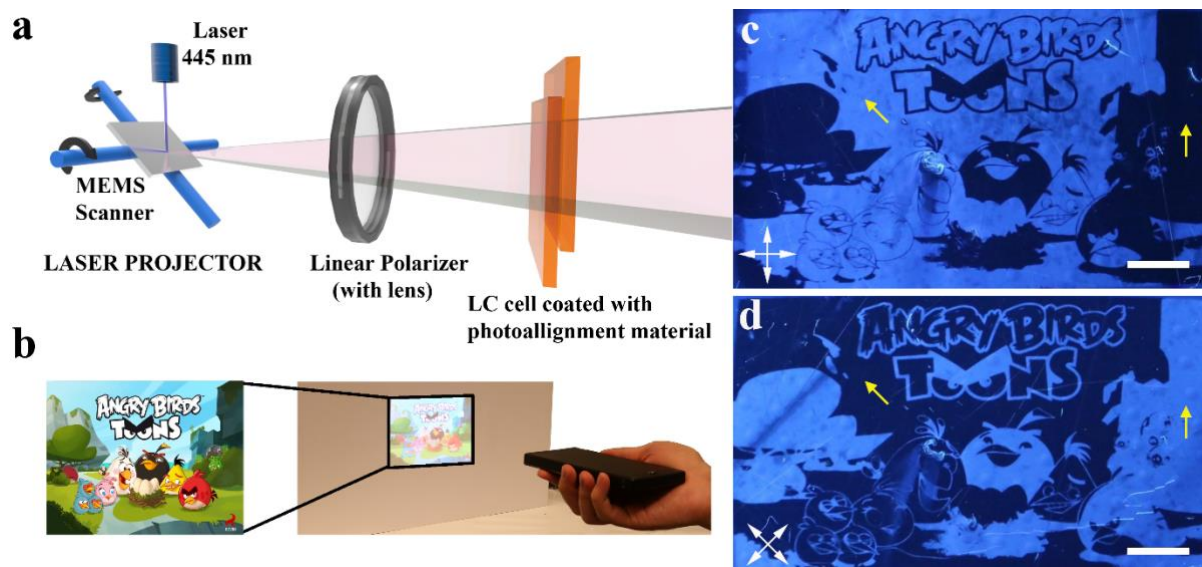


**Figure 1.** (a) Working principle of the photoalignment set-up with the single-mirror MEMS laser projector. (b) Projection of a coloured image by the miniature laser projector. (c) and (d) Polarized microscope images of photopatterned samples. Crossed double-headed arrows represent the polarizer and analyser directions, yellow arrows indicate the local LC alignment orientation. Scale bars: 3 mm. Image in (b) used with permission from Rovio Entertainment Ltd.

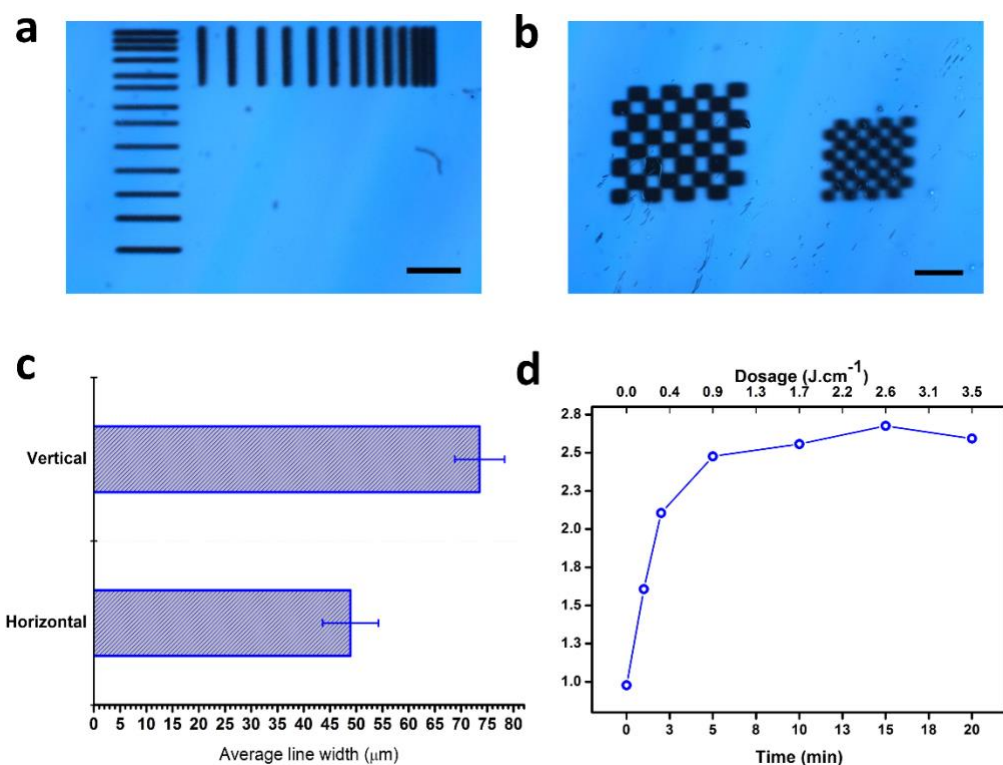


**Figure 2.** (a) Polarized optical images of lines patterned in the horizontal and vertical directions. (b) Polarized optical image of checkerboard patterns showing the minimum pixel size while maintaining high resolution and contrast. (c) Minimum line widths that can be patterned in the vertical and horizontal directions (error bars indicate standard deviation for 10 independent measurements). (d) Dichroic ratio vs. time/light dose during incident on the sample during the patterning illumination. Scale bars in (a) and (b) correspond to  $500\ \mu\text{m}$ .



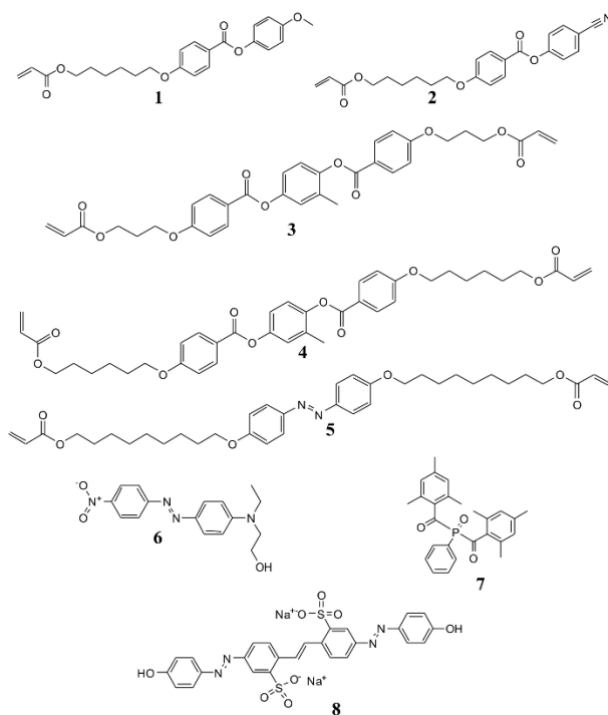


**Figure 3.** Chemical structures of the compounds used in this work.

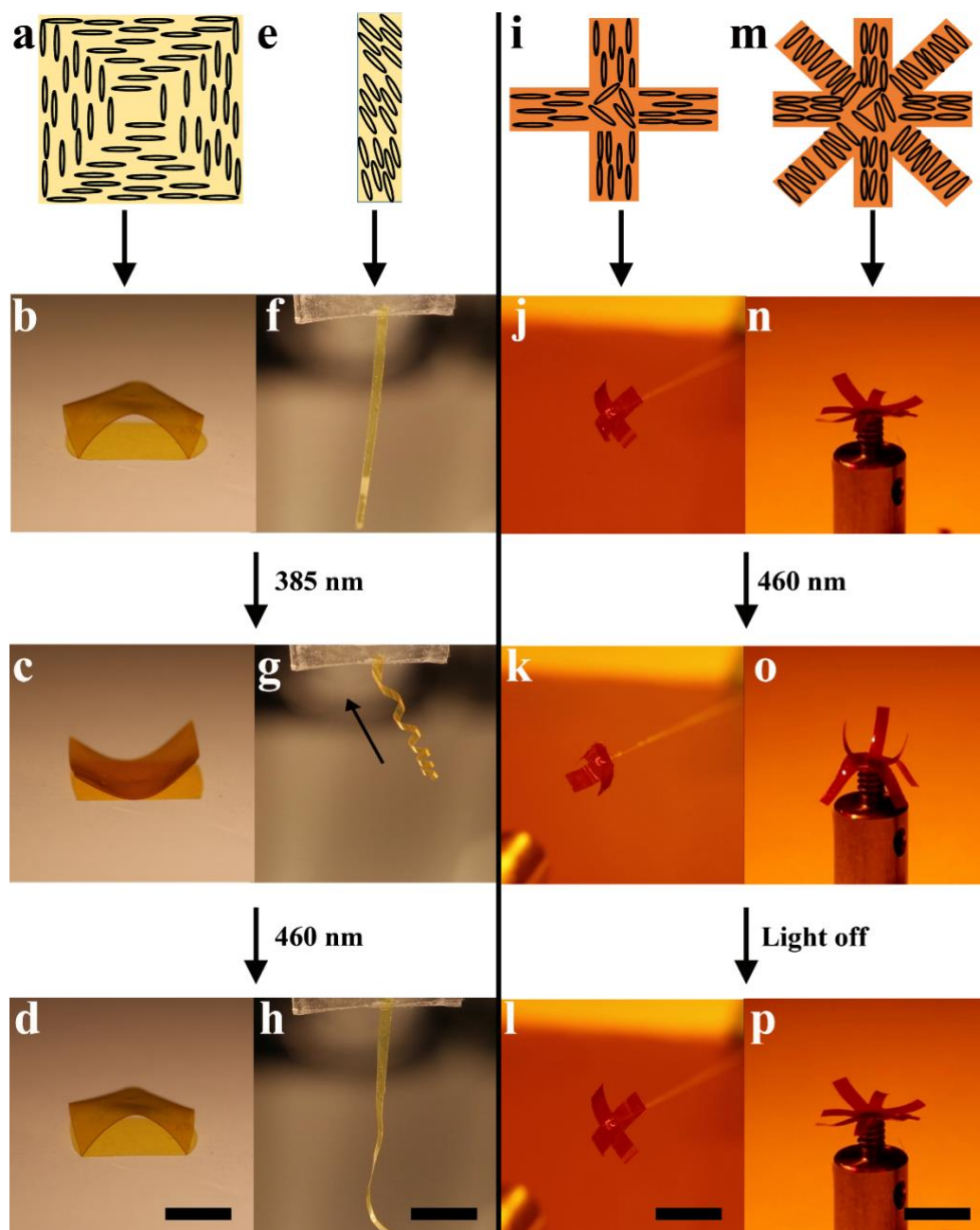


**Figure 4.** Molecular orientation and actuation via photochemical mechanism of (a-d) a film with +1 topological defect; (e-h) a film stripe with modified director angles from one end to the other. Photothermally actuated 4-armed gripper (i-l), and 8-legged "insect" structure (m-p). All scale bars correspond to 6 mm.

**Programmed photo-responses** are inscribed into monolithic actuators made of liquid crystal polymer networks, using a laser projector and photoalignment technique. We demonstrate distinct light-induced shape changes, such as bending, buckling, coiling, gripping and octopus-like motion, driven by both photochemical and photothermal actuation. The reported technique enables easy and efficient programming in actuation, thereby significantly facilitating the realization of functional soft robots.

O. M. Wani, H. Zeng,\* P. Wasylczyk and A. Priimagi\*

**Programming photo-response in liquid crystal polymer actuators with laser projector**

